

1 **Genome-wide association studies of autoimmune vitiligo identify 23 new risk loci and**
2 **highlight key pathways and regulatory variants**

3

4 Ying Jin^{1,2}, Genevieve Andersen¹, Daniel Yorgov³, Tracey M Ferrara¹, Songtao Ben¹, Kelly M
5 Brownson¹, Paulene J Holland¹, Stanca A Birlea^{1,4}, Janet Siebert⁵, Anke Hartmann⁶, Anne Lienert⁶, Nanja
6 van Geel⁷, Jo Lambert⁷, Rosalie M Luiten⁸, Albert Wolkerstorfer⁸, JP Wietze van der Veen^{8,9}, Dorothy C
7 Bennett¹⁰, Alain Taïeb¹¹, Khaled Ezzedine¹¹, E Helen Kemp¹², David J Gawkrödger¹², Anthony P
8 Weetman¹², Sulev Kõks¹³, Ele Prans¹³, Külli Kingo¹⁴, Maire Karelson¹⁴, Margaret R Wallace¹⁵, Wayne T
9 McCormack¹⁶, Andreas Overbeck¹⁷, Silvia Moretti¹⁸, Roberta Colucci¹⁸, Mauro Picardo¹⁹, Nanette B
10 Silverberg^{20,21}, Mats Olsson²², Yan Valle²³, Igor Korobko^{23,24}, Markus Böhm²⁵, Henry W. Lim²⁶, Iltefat
11 Hamzavi²⁶, Li Zhou²⁶, Qing-Sheng Mi²⁶, Pamela R. Fain^{1,2}, Stephanie A Santorico^{1,3,27}, & Richard A
12 Spritz^{1,2}

13

14 ¹Human Medical Genetics and Genomics Program and ²Department of Pediatrics, University of
15 Colorado School of Medicine, Aurora, Colorado, USA. ³Department of Mathematical and
16 Statistical Sciences, University of Colorado Denver, Denver, Colorado, USA. ⁴Department of
17 Dermatology, University of Colorado School of Medicine, Aurora, Colorado, USA.
18 ⁵CytoAnalytics, Denver, Colorado, USA. Department of Dermatology, ⁶University Hospital
19 Erlangen, Erlangen, Germany. ⁷Department of Dermatology, Ghent University Hospital, Ghent,
20 Belgium. ⁸Netherlands Institute for Pigment Disorders, Department of Dermatology, Academic
21 Medical Centre University of Amsterdam, Amsterdam, The Netherlands. ⁹Department of
22 Dermatology, Medical Centre Haaglanden, The Hague, The Netherlands. ¹⁰Molecular & Clinical
23 Sciences Research Institute, St. George's, University of London, London, UK. ¹¹Centre de
24 Référence des maladies rares de la peau, Department of Dermatology, Hôpital St.-André,
25 Bordeaux, France. ¹²Department of Oncology and Metabolism, University of Sheffield,

26 Sheffield, UK. ¹³Department of Pathophysiology and ¹⁴Department of Dermatology, University of
27 Tartu, Tartu, Estonia. ¹⁵Department of Molecular Genetics & Microbiology, and ¹⁶Department of
28 Pathology, Immunology, and Laboratory Medicine, University of Florida College of Medicine,
29 Gainesville, Florida, USA. ¹⁷Lumiderm, Madrid, Spain. ¹⁸Section of Dermatology, Department of
30 Surgery and Translational Medicine, University of Florence, Italy. ¹⁹Laboratorio Fisiopatologia
31 Cutanea, Istituto Dermatologico San Gallicano, Rome, Italy. ²⁰Department of Dermatology,
32 Columbia University College of Physicians and Surgeons, New York, New York, USA and
33 ²¹Pediatric and Adolescent Dermatology, St. Luke's-Roosevelt Hospital Center, New York, New
34 York, USA. ²²International Vitiligo Center, Uppsala, Sweden. ²³Vitiligo Research Foundation,
35 New York, New York, USA. ²⁴Institute of Gene Biology, Russian Academy of Sciences,
36 Moscow, Russia. ²⁵Department of Dermatology, University of Münster, Münster, Germany.
37 ²⁶Department of Dermatology, Henry Ford Hospital, Detroit, Michigan, USA. ²⁷Department of
38 Biostatistics and Informatics, Colorado School of Public Health, University of Colorado, Aurora,
39 Colorado, USA.

40

41 Correspondence should be addressed to R.A.S. (richard.spritz@ucdenver.edu).

42

43

44

45 **Vitiligo is an autoimmune disease in which depigmented skin results from destruction of**
46 **melanocytes¹, with epidemiologic association with other autoimmune diseases². In**
47 **previous linkage and genome-wide association studies (GWAS1, GWAS2), we identified**
48 **27 vitiligo susceptibility loci in patients of European (EUR) ancestry. We carried out a**
49 **third GWAS (GWAS3) in EUR subjects, with augmented GWAS1 and GWAS2 controls,**
50 **genome-wide imputation, and meta-analysis of all three GWAS, followed by an**
51 **independent replication. The combined analyses, with 4,680 cases and 39,586 controls,**
52 **identified 23 new loci and 7 suggestive loci, most encoding immune and apoptotic**
53 **regulators, some also associated with other autoimmune diseases, as well as several**
54 **melanocyte regulators. Bioinformatic analyses indicate a predominance of causal**
55 **regulatory variation, some corresponding to eQTL at these loci. Together, the identified**
56 **genes provide a framework for vitiligo genetic architecture and pathobiology, highlight**
57 **relationships to other autoimmune diseases and melanoma, and offer potential targets**
58 **for treatment.**

59

60 In previous genome-wide linkage and association studies, we identified 27 vitiligo susceptibility loci³⁻⁶ in
61 EUR subjects, principally encoding immunoregulatory proteins, many of which are associated with other
62 autoimmune diseases⁷. Several other vitiligo-associated genes encode melanocyte components that
63 regulate normal pigmentary variation⁸ and in some cases are major vitiligo autoimmune antigens, with an
64 inverse association of variation at these loci with vitiligo *versus* malignant melanoma^{4,6}. To detect
65 additional vitiligo-associations with lower odds ratios (ORs), as well as uncommon risk alleles with
66 higher ORs, we conducted a third GWAS (GWAS3) of EUR subjects. We augmented the number of
67 population controls in our previous GWAS1 and GWAS2 and performed genome-wide imputation of all
68 three EUR vitiligo GWAS. After quality control procedures, the augmented studies included 1,381 cases
69 and 14,518 controls (GWAS1), 413 cases and 5,209 controls (GWAS2), and 1,059 cases and 17,678
70 controls (GWAS3), with genomic inflation factors 1.068, 1.059, and 1.013, respectively. We performed a

71 fixed-effects meta-analysis of the three GWAS datasets for 8,966,411 markers (GWAS123; Online
72 Methods). Replication used an additional 1,827 EUR vitiligo cases and 2,181 controls.

73 Results for the three individual GWAS, the meta-analysis, and the replication study are presented
74 in **Table 1, Supplementary Table 1, and Fig. 1**. Twenty-three new loci achieved genome-wide
75 significance ($P < 5 \times 10^{-8}$) for association with vitiligo and demonstrated subsequent replication; of these,
76 21 are completely novel (*FASLG*, *PTPRC*, *PPP4R3B*, *BCL2L11*, *FARP2-STK25*, *UBE2E2*, *FBXO45*-
77 *NRROS*, *PPP3CA*, *IRF4*, *SERPINB9*, *CPVL*, *NEK6*, *ARID5B*, a multigenic segment that includes *BAD*,
78 *TNFSF11*, *KAT2A-HSPB9-RAB5C*, *TNFRSF11A*, *SCAF1-IRF3-BCL2L12*, a multigenic segment that
79 includes *ASIP*, *PTPN1*, and *IL1RAPL1*), while two, *CTLA4* and *TICAM1*, were suggestive in our previous
80 studies. One previously significant locus, *CLNK*, was no longer significant (**Supplementary Table 1**).
81 Another potential new locus, *PVTI*, exceeded genome-wide significance in the discovery meta-analysis
82 ($P = 7.74 \times 10^{-9}$), but could not be successfully genotyped in the replication study and so remains
83 uncertain. Two other loci, *FLII* and *LOC101060498*, exceeded genome-wide significance in the
84 discovery meta-analysis ($P = 3.76 \times 10^{-8}$ and $P = 3.60 \times 10^{-11}$, respectively), but did not demonstrate
85 replication. Seven additional novel loci achieved suggestive significance ($P < 10^{-5}$) in the discovery meta-
86 analysis (*STAT4*, *PPARGC1B*, *c7orf72*, *PARP12*, *FADS2*, *CBFA2T3*, and a chr17 locus in the vicinity of
87 *AFMID*) and gave evidence of replication, but failed to achieve genome-wide significance
88 (**Supplementary Table 1**).

89 Together, the most significantly associated variants at the 48 loci (**Table 1**) identified by meta-
90 analyses of the three GWAS account for 17.4% of vitiligo heritability ($h^2 \sim 0.75$). To assess whether
91 additional independent variants at these loci might account for additional vitiligo heritability, we
92 performed logistic regression conditional on the most significant SNP at each locus. Eight loci (*FARP2*-
93 *STK25*, *IFIH1*, *IL2RA*, *LPP*, *MC1R*, *SLA/TG*, *TYR*, *UBASH3A*) and the MHC showed evidence of
94 additional independent associations, accounting for an additional 5.1% of vitiligo heritability, for a total
95 of 22.5%. In general, the ORs for the 23 new confirmed loci were lower than those for loci detected
96 previously⁶, 1.15 to 1.27, excepting *CPVL* (OR = 1.84), *RALY-EIF252-ASIP-AHCY-ITCH* (OR = 1.64),

97 and *IL1RAPL1* (OR = 1.77); for these three signals the associated alleles are uncommon (minor allele
98 frequencies 0.03, 0.07, and 0.01, respectively) and thus were not detected in the previous GWAS due to
99 power limitations.

100 To screen for functional relationships among proteins encoded at the 48 confirmed vitiligo-
101 associated loci, we included all genes under the association peaks at these loci in unsupervised pathway
102 analyses using g:PROFILER⁹, PANTHER¹⁰, and STRING¹¹. PANTHER and gPROFILER identified an
103 enriched network of BioGRID interactions, most significant for the GO categories immune response,
104 immune system process, positive regulation of response to stimulus, positive regulation of biological
105 process, and regulation of response to stimulus. STRING identified a large potential interaction network
106 (**Fig. 2**), with a predominance of proteins involved in immunoregulation, T-cell receptor repertoire,
107 apoptosis, antigen processing and presentation, and melanocyte function.

108 Considering proteins encoded at the 23 newly confirmed vitiligo candidate loci, at least twelve
109 (CTLA4, TICAM1, PTPRC, FARP2, UBE2E2, NRROS, CPVL, ARID5B, PTPN1, TNFSF11,
110 TNFRSF11A, IRF3, and perhaps also *IL1RAPL1*) play roles in immune regulation, and PPP3CA may
111 regulate FOXP3 via NFATC2 and is associated with canine lupus¹². Six (FASLG, BCL2L11, BCL2L12,
112 SERPINB9, NEK6, BAD) are regulators of apoptosis, particularly involving immune cells. ASIP is a
113 regulator of melanocyte gene expression, and IRF4 is a key transcription factor for both immune cells and
114 melanocytes.

115 Strikingly, several vitiligo-associated genes encode proteins that interact physically and
116 functionally. BCL2L11 and BAD are binding partners that promote apoptosis¹³. CD80 binds to CTLA4 to
117 inhibit T cell activation¹⁴. BCL2L12 binds to and neutralizes caspase 7 (*CASP7*)¹⁵. SERPINB9 binds to
118 and specifically inhibits granzyme B (*GZMB*)¹⁶. Eos (*IKZF4*) binds and is an obligatory co-repressor of
119 FOXP3 in regulatory T cells¹⁷. RANK (*TNFRSF11A*) binds to RANKL (*TNFSF11*) to regulate many
120 aspects of immune cell function, including interactions of T cells and dendritic cells and thymic
121 tolerization¹⁸. Agouti signaling protein (*ASIP*) binds to the melanocortin-1 receptor (*MC1R*) to down-
122 regulate production of brown-black eumelanin¹⁹. IRF4 cooperates with MITF to activate transcription of

123 *TYR*²⁰. And the vitiligo-associated *HLA-A*02:01:01:01* subtype presents peptide antigens derived from
124 several different melanocyte proteins, including tyrosinase (*TYR*), *OCA2*, and *MC1R*^{4,6,21}. Together, these
125 relationships appear to highlight key pathways of vitiligo pathogenesis that are beginning to coalesce.

126 An unexpected finding from vitiligo GWAS has been an inverse relationship between vitiligo and
127 malignant melanoma risk for genes that encode melanocyte structural and regulatory proteins. *TYR*,
128 *OCA2*, and *MC1R*, encode functional components of the melanocyte and are key vitiligo autoantigens.
129 *IRF4* encodes a transcription factor for melanocytes as well as lymphoid, myeloid, and dendritic cells²²,
130 controlled by alternative tissue-specific enhancers²³. *ASIP* and *PPARGC1B* encode paracrine regulators of
131 melanocyte gene expression. All six loci play important roles in normal pigimentary variation^{8,24}, and for
132 all six the specific SNPs associated with vitiligo risk are also associated with melanoma protection, and
133 *vice-versa*²⁵⁻²⁷. The inverse genetic relationship of susceptibility to vitiligo *versus* melanoma suggests that
134 vitiligo may represent enhanced immune surveillance against melanoma^{27,28}, consistent with the threefold
135 reduction in melanoma incidence among vitiligo patients^{29,30} and prolonged survival of melanoma patients
136 who develop vitiligo during immunotherapy³¹.

137 Vitiligo is epidemiologically associated with several other autoimmune diseases, including
138 autoimmune thyroid disease, pernicious anemia, rheumatoid arthritis, adult-onset type 1 diabetes,
139 Addison's disease, and lupus^{2,32}. We searched the NHGRI-EBI GWAS Catalog and PubMed for the 48
140 genome-wide significant and 7 suggestive vitiligo susceptibility loci for associations with other
141 autoimmune, inflammatory, and immune-related disorders. As shown in **Fig. 3**, of the 23 novel genome-
142 wide significant vitiligo loci, *FASLG* has been associated with celiac disease³³ and Crohn's disease³⁴;
143 *PTPRC* with ulcerative colitis³⁵; *BCL2L11* with primary sclerosing cholangitis³⁶; *CTLA4* with alopecia
144 areata³⁷, rheumatoid arthritis³⁸, autoimmune thyroid disease^{39,40}, myasthenia gravis⁴¹, and type 1 diabetes
145 autoantibody production⁴²; *TNFRSF11A* with myasthenia gravis⁴¹; and *ARID5B* with systemic lupus
146 erythematosus⁴³. Of the seven suggestive loci, *STAT4* has been associated with Behçet's disease⁴⁴,
147 Sjögren's syndrome⁴⁵, and lupus⁴⁶; and *c7orf72* with lupus⁴⁷. These concordant associations for vitiligo
148 and other autoimmune and inflammatory diseases add to those involving previously identified vitiligo

149 susceptibility loci, which include *RERE*, *PTPN22*, *IFIH1*, *CD80*, *LPP*, *BACH2*, *RNASET2-FGFR1OP-*
150 *CCR6*, *TG/SLA*, *IL2RA*, *CD44*, a chr11q21 gene desert, *IKZF4*, *SH2B3-ATXN2*, *UBASH3A*, and
151 *CIQTNF6*^{4,6}. Nevertheless, in most cases it remains uncertain whether apparent shared locus associations
152 for different autoimmune diseases reflect shared or different underlying causal variants.

153 A majority of loci associated with complex traits involve causal variants that are regulatory in
154 nature⁴⁸⁻⁵², often corresponding to apparent expression quantitative trait loci (eQTLs)⁵². For *TYR*²¹,
155 *GZMB*⁵³, and *MC1R*⁷, principal vitiligo risk derives from missense substitutions, whereas for *OCA2*⁶ and
156 the MHC class I⁵⁴ and class II⁵⁵ loci principal vitiligo risk is associated with causal variation in nearby
157 transcriptional regulatory elements. To assess the fraction of vitiligo-associated loci for which causal
158 variation is likely regulatory, we carried out conditional logistic regression analysis of all loci to define
159 independent association signals, and for each signal we compiled all variants that could not be statistically
160 distinguished. All variants were then annotated against all available ENCODE datasets for immune-
161 related and melanocyte-related cells (**Supplementary Table 2**). Overall, at approximately 58% of loci,
162 the most significant variants (or statistically indistinguishable variants) are within a transcriptional
163 regulatory element predicted by ENCODE data^{56,57}. Only about 15% are in coding regions, several
164 resulting in missense substitutions. To further assess the general functional categories of apparent causal
165 variants for vitiligo, we applied stratified LD score regression⁵¹ to the GWAS meta-analysis summary
166 statistics. As shown in **Fig. 4**, greatest enrichment of heritability was observed for markers in regulatory
167 functional categories, with considerably less enrichment of markers in protein coding regions.

168 We utilized two approaches to assess correspondence of vitiligo association signals with
169 expression of genes in the vicinity. We used PrediXcan⁵⁸ to predict expression of 11,553 genes in whole
170 blood for each study subject and then tested association of predicted expression of each gene with vitiligo
171 affection status. We used a Bayesian method to assess co-localization of *cis* eQTL signals in purified
172 blood monocytes with the confirmed vitiligo association signals. The PrediXcan analysis found 83 genes
173 with significant differential predicted expression in vitiligo cases versus controls after Bonferroni
174 correction (**Supplementary Table 3**); of these, 75 were located within 1 Mb of one of the 48 confirmed

175 vitiligo susceptibility loci, demonstrating highly significant enrichment compared with locations of genes
176 non-significant for PrediXcan (P value < 0.00001). The eQTL analysis found that 8 of the confirmed
177 vitiligo association signals showed significant co-localization with eQTL association signals identified in
178 purified monocytes (**Supplementary Fig. 1** and **Supplementary Table 4**). Of the confirmed vitiligo-
179 associated genes that could be tested using both methods, 6 were significant in both analyses (*CASP7*,
180 *HERC2-OCA2*, *ZC3H7B-TEF*, *TICAM1*, *RERE*, *RNASET2-FGFR1OP-CCR6*). For all of these except
181 *CASP7*, one or more of the most associated SNPs not distinguishable by logistic regression was located
182 within or very close to an ENCODE element likely to regulate gene expression in immune cell types,
183 melanocytes, or both (**Supplementary Table 2**).

184 Like a jigsaw puzzle, the pieces of the vitiligo pathogenome are thus beginning to fit together,
185 revealing a complex network of immunoregulatory proteins, apoptotic regulators, and melanocyte
186 components that mediate both autoimmune targeting of melanocytes in vitiligo and susceptibility to
187 melanoma. For vitiligo as for other complex diseases, there is enrichment of causal variation in regions
188 that regulate gene expression. This may bode well for identifying potential therapeutic targets, as
189 pharmacologic modulation of dysregulated biological pathways may prove more tractable than attempting
190 to target proteins impacted by amino acid substitutions.

191

192

193 **URLs.** 1000 Genomes Project, <http://www.1000genomes.org/>; 1000 Genomes Project data,
194 <http://www.sph.umich.edu/csg/abecasis/MACH/download/1000G-2010-08.html>; NHGRI-EBI GWAS
195 Catalog, <http://www.ebi.ac.uk/gwas/>; NIH Database of Genotypes and Phenotypes (dbGaP),
196 <http://www.ncbi.nlm.nih.gov/gap>; Online Mendelian Inheritance in Man (OMIM),
197 <http://www.ncbi.nlm.nih.gov/omim>; PLINK, <http://pngu.mgh.harvard.edu/purcell/plink/>; STATA,
198 <http://www.stata.com>; STRING database, <http://string-db.org>.

199

200 **Accession Codes.** Genotype and phenotype data for GWAS1, GWAS2, and GWAS 3 have been
201 deposited with the NIH Database of Genotypes and Phenotypes (dbGaP) as phs000224.v1.p1,
202 phs000224.v2.p1, and phs000224.v3.p1, respectively.

203

204 **ACKNOWLEDGMENTS**

205 We thank the thousands of vitiligo patients and normal control individuals around the world who
206 participated in this study. We thank the Center for Inherited Disease Research (CIDR) for genotyping.
207 This work utilized the Janus supercomputer, which is supported by the National Science Foundation
208 (award number CNS-0821794), the University of Colorado Boulder, the University of Colorado Denver,
209 and the National Center for Atmospheric Research. The Janus supercomputer is operated by the
210 University of Colorado Boulder. This work was supported by grants R01AR045584, R01AR056292,
211 X01HG007484, and P30AR057212 from the U.S. National Institutes of Health and by institutional
212 research funding IUT20-46 from the Estonian Ministry of Education and Research.

213

214 **AUTHOR CONTRIBUTIONS**

215 Y.J., G.A. and D.Y. performed statistical analyses. J.S. managed computer databases, software, and
216 genotype data. T.M.F., S.B., G.A., and K.M.B. managed DNA samples and contributed to experimental
217 procedures. P.J.H. managed subject coordination. S.A.B., A.H., A.L., R.M.L., A.W., J.P.W.vdV., N.vG.,
218 J.L., D.C.B., A.T., K.E., E.H.K., D.J.G., A.P.W., S.K., E.P., K.K., M.K., M.R.W., W.T.M., A.O., S.M.,
219 R.C., M.P., N.B.S., M.S., Y.V., I.K., M.B., H.L., I.H., L.Z., and Q.-S.M. provided subject samples and
220 phenotype information. S.A.S., P.R.F. and R.A.S. conceived, oversaw, and managed all aspects of the
221 study. R.A.S. wrote the first draft of the manuscript. All authors contributed to the final paper.

222

223

224

225 **References (Main text)**

- 226 1. Picardo, M. & Taïeb, A. (eds.) Vitiligo (Springer, Heidelberg & New York, 2010).
- 227 2. Alkhateeb, A. *et al.* Epidemiology of vitiligo and associated autoimmune diseases in
228 Caucasian probands and their families. *Pigment Cell Res.* **16**, 208–214 (2003).
- 229 3. Jin, Y. *et al.* *NALP1* in vitiligo-associated multiple autoimmune disease. *N. Engl. J. Med.*
230 **356**, 1216-1225 (2007).
- 231 4. Jin, Y. *et al.* Variant of *TYR* and autoimmunity susceptibility loci in generalized vitiligo. *N.*
232 *Engl. J. Med.* **362**, 1686–1697 (2010).
- 233 5. Jin, Y. *et al.* Common variants in *FOXP1* are associated with generalized vitiligo. *Nat.*
234 *Genet.* **42**, 576-578 (2010).
- 235 6. Jin, Y. *et al.* Genome-wide association study and meta-analysis identifies 13 new
236 melanocyte-specific and immunoregulatory susceptibility loci for generalized vitiligo. *Nat.*
237 *Genet.* **44**, 676-680 (2012).
- 238 7. Ricano-Ponce I & Wijmenga C. Mapping of immune-mediated disease genes. *Annu. Rev.*
239 *Genomics Hum. Genet.* **14**, 325–353 (2013).
- 240 8. Liu F. *et al.* Genetics of skin color variation in Europeans: genome-wide association studies
241 with functional follow-up. *Hum Genet.* **134**, 823–835 (2015).
- 242 9. Reimand, J., Arak, T. & Vilo J. g:Profiler—a web server for functional interpretation of gene
243 lists (2011 update). *Nucleic Acids Res.*, **39**, W307-15 (2011).
- 244 10. Mi, H., Poudel, S., Muruganujan, A., Casagrande, J.T. & Thomas P.D. PANTHER version
245 10: expanded protein families and functions, and analysis tools. *Nucleic. Acids. Res.* **44**,
246 D336-342 (2016).
- 247 11. Szklarczyk, D. *et al.* STRING v10: protein-protein interaction networks, integrated over the
248 tree of life. *Nucleic Acids Res.* **43**, D447-D452 (2015).
- 249 12. Wilbe, M., *et al.* Multiple changes of gene expression and function reveal genomic and
250 phenotypic complexity in SLE-like disease. *PLoS Genet.* **11**, e1005248 (2015).

- 251 13. Wang, X., Xing, D., Liu, L. & Chen, W.R. BimL directly neutralizes Bcl-xL to promote Bax
252 activation during UV-induced apoptosis. *FEBS Lett.* **583**, 1873-1879 (2009).
- 253 14. Linsley, P.S. *et al.* Human B7-1 (CD80) and B7-2 (CD86) bind with similar avidities but
254 distinct kinetics to CD28 and CTLA-4 receptors. *Immunity.* **1**, 793-801 (1994).
- 255 15. Stegh, A.H. *et al.* Bcl2L12 inhibits post-mitochondrial apoptosis signaling in glioblastoma.
256 *Genes Dev.* **21**, 98-111 (2007).
- 257 16. Sun, J. *et al.* A cytosolic granzyme B inhibitor related to the viral apoptotic regulator cytokine
258 response modifier A is present in cytotoxic lymphocytes. *J. Biol. Chem.* **271**, 27802-27809
259 (1996).
- 260 17. Pan, F. *et al.* Eos mediates Foxp3-dependent gene silencing in CD4+ regulatory T cells.
261 *Science* **325**, 1142-1146 (2009).
- 262 18. Akiyama, T., Shinzawa, M., & Akiyama, N. RANKL-RANK interaction in immune regulatory
263 systems. *World J. Orthop.* **3**, 142-150 (2012).
- 264 19. Ollmann, M.M., Lamoreux, M.L., Wilson, B.D. & Barsh, G.S. Interaction of Agouti protein
265 with the melanocortin 1 receptor in vitro and in vivo. *Genes Dev.* **12**, 316-330 (1998).
- 266 20. Praetorius, C. *et al.* A polymorphism in IRF4 affects human pigmentation through a
267 tyrosinase-dependent MITF/TFAP2A pathway. *Cell* **155**, 1022-1033 (2013).
- 268 21. Jin, Y. *et al.* Next-generation DNA re-sequencing identifies common variants of *TYR* and
269 *HLA-A* that modulate the risk of generalized vitiligo via antigen presentation. *J. Invest.*
270 *Dermatol.* **132**, 1730-1733 (2012).
- 271 22. Gualco, G., Weiss, L.M. & Bacchi, C.E. MUM1/IRF4. A review. *Appl. Immunohistochem. Mol.*
272 *Morphol.* **18**, 301-310 (2010).
- 273 23. Visser, M., Palstra, R.J. & Kayser, M. Allele-specific transcriptional regulation of IRF4 in
274 melanocytes is mediated by chromatin looping of the intronic rs12203592 enhancer to the
275 *IRF4* promoter. *Hum. Mol. Genet.* **25**, 2629-2661 (2015).

- 276 24. Nan H. *et al.* Genome-wide association study of tanning phenotype in a population of
277 European ancestry. *J. Invest. Dermatol.* **129**, 2250-2257 (2009).
- 278 25. Shoag, J. *et al.* PGC-1 coactivators regulate MITF and the tanning response. *Mol. Cell* **49**,
279 145-157. (2013).
- 280 26. Read, J., Wadt, K.A. & Hayward, N.K. Melanoma genetics. *J. Med. Genet.* **53**, 1-14 (2016).
- 281 27. Spritz, R.A. The genetics of generalized vitiligo: autoimmune pathways and an inverse
282 relationship with malignant melanoma. *Genome Med.* **19**, 2:78 (2010).
- 283 28. Das, P.K., van den Wijngaard R.M.J.G.J., Wankowicz-Kalinska, A. & Le Poole, I.C. A
284 symbiotic concept of autoimmunity and tumour immunity: lessons from vitiligo. *Trends*
285 *Immunol.* **22**, 130-136 (2001).
- 286 29. Teulings, H.E. *et al.* Decreased risk of melanoma and nonmelanoma skin cancer in patients
287 with vitiligo: a survey among 1307 patients and their partners. *Br. J. Dermatol.* **168**, 162-171
288 (2013).
- 289 30. Paradisi, A. *et al.* Markedly reduced incidence of melanoma and nonmelanoma skin cancer
290 in a nonconcurrent cohort of 10040 patients with vitiligo. *J. Am. Acad. Dermatol.* **71**, 1110-
291 1116 (2014).
- 292 31. Teulings, H.E. *et al.* Vitiligo-like depigmentation in patients with stage III-IV melanoma
293 receiving immunotherapy and its association with survival: a systematic review and meta-
294 analysis. *J. Clin Onc.* **33**, 773-781 (2015).
- 295 32. Laberge, G. *et al.* Early disease onset and increased risk of other autoimmune diseases in
296 familial generalized vitiligo. *Pigment Cell Res.* **18**, 300-305 (2005).
- 297 33. Dubois, P.C. *et al.* Multiple common variants for celiac disease influencing immune gene
298 expression. *Nat. Genet.* **42**, 295-302 (2010).
- 299 34. Franke A. *et al.* Genome-wide meta-analysis increases to 71 the number of confirmed
300 Crohn's disease susceptibility loci. *Nat. Genet.* **42**, 1118-1125 (2010).

- 301 35. Juyal, G. *et al.* Genome-wide association scan in north Indians reveals three novel HLA-
302 independent risk loci for ulcerative colitis. *Gut* **64**, 571-579 (2015).
- 303 36. Melum E. *et al.* Genome-wide association analysis in primary sclerosing cholangitis
304 identifies two non-HLA susceptibility loci. *Nat. Genet.* **43**, 17-19 (2011).
- 305 37. Petukhova, L. *et al.* Genome-wide association study in alopecia areata implicates both
306 innate and adaptive immunity. *Nature* **466**, 113-117 (2010).
- 307 38. Gregersen, P.K. *et al.* REL, encoding a member of the NF-kappaB family of transcription
308 factors, is a newly defined risk locus for rheumatoid arthritis. *Nat. Genet.* **41**, 820-823
309 (2009).
- 310 39. Chu, X. *et al.* A genome-wide association study identifies two new risk loci for Graves'
311 disease. *Nat. Genet.* **43**, 897-901 (2011).
- 312 40. Eriksson, N. *et al.* Novel associations for hypothyroidism include known autoimmune risk
313 loci. *PLoS One* **7**, e34442 (2012).
- 314 41. Renton, A.E. *et al.* A genome-wide association study of myasthenia gravis. *JAMA Neurol.*
315 **72**, 396-404 (2015).
- 316 42. Plagnol, V. *et al.* Genome-wide association analysis of autoantibody positivity in type 1
317 diabetes cases. *PLoS Genet.* **7**, e1002216 (2011).
- 318 43. Yang, W. *et al.* Meta-analysis followed by replication identifies loci in or near CDKN1B,
319 TET3, CD80, DRAM1, and ARID5B as associated with systemic lupus erythematosus in
320 Asians. *Am. J. Hum. Genet.* **92**, 41-51 (2013).
- 321 44. Hou, S. *et al.* Identification of a susceptibility locus in STAT4 for Behcet's disease in Han
322 Chinese in a genome-wide association study. *Arth. Rheumat.* **64**, 4104-4113 (2012).
- 323 45. Li, Y. *et al.* A genome-wide association study in Han Chinese identifies a susceptibility locus
324 for primary Sjogren's syndrome at 7q11.23. *Nat. Genet.* **45**, 1361-1365 (2013).

- 325 46. Lee, Y.H., Bae, S.C., Choi, S.J., Ji, J.D. & Song, G.G. Genome-wide pathway analysis of
326 genome-wide association studies on systemic lupus erythematosus and rheumatoid arthritis.
327 *Molec. Biol. Rep.* **39**, 10627-10635 (2012).
- 328 47. Han, J.W. *et al.* Genome-wide association study in a Chinese Han population identifies nine
329 new susceptibility loci for systemic lupus erythematosus. *Nat. Genet.* **41**, 1234-1237 (2009).
- 330 48. Corradin, O. & Schcheri, P.C. Enhancer variants: evaluating functions in common disease.
331 *Genome Med.* **6**, 85 (2014).
- 332 49. Gusev, A. *et al.* Partitioning heritability of regulatory and cell-type-specific variants across 11
333 common diseases. *Am. J. Hum. Genet.* **95**, 535-552 (2014).
- 334 50. Paul, D.S. *et al.* Functional interpretation of non-coding sequence variation: concepts and
335 challenges. *Bioessays* **36**, 191-199 (2014).
- 336 51. Finucane, H.K. *et al.* Partitioning heritability by functional annotation using genome-wide
337 association summary statistics. *Nat. Genet.* **47**, 1228-1235 (2015).
- 338 52. Nicolae, D. *et al.* Trait-associated SNPs are more likely to be eQTLs: annotation to enhance
339 discovery from GWAS. *PLoS Genet.* **6**, e1000888 (2010).
- 340 53. Ferrara, T.M., Jin, Y., Gowan, K., Fain, P.R., & Spritz, R.A. Risk of generalized vitiligo is
341 associated with the common 55R-94A-247H variant haplotype of *GZMB* (encoding
342 Granzyme B). *J. Investig. Dermatol.* **133**, 1677-1679 (2013).
- 343 54. Hayashi, M. *et al.* Autoimmune vitiligo is associated with gain of function by a transcriptional
344 regulator that elevates expression of HLA-A*02:01 *in vivo*. *Proc. Natl. Acad. Sci. U.S.A.* **113**,
345 1357-1362 (2016).
- 346 55. Cavalli, G. *et al.* MHC class II super-enhancer increases surface expression of HLA-DR and
347 HLA-DQ and affects cytokine production in autoimmune vitiligo. *Proc. Natl. Acad. Sci. U.S.A.*
348 **113**, 1363-1368 (2016).
- 349 56. Shlyueva, D., Stampfel, G. & Stark, A. Transcriptional enhancers from properties to
350 genome-wide predictions. *Nat. Rev. Genet.* **15**, 272-286 (2014).

- 351 57. Kellis, M. *et al.* Defining functional DNA elements in the human genome. *Proc. Natl. Acad.*
352 *Sci. U.S.A.* **111**, 6131–6138 (2014).
- 353 58. Gamazon, E.R. *et al.* A gene-based association method for mapping traits using reference
354 transcriptome data. *Nat. Genet.* **47**, 1091-1098 (2015).

355

356

357 **Figure Legends (Main text)**

358

359 **Figure 1** Genome-wide meta-analysis results. The genome-wide distribution of $-\log_{10}(P \text{ values})$
360 from the Cochran-Mantel-Haenszel meta-analysis for 8,966,411 genotyped and imputed
361 markers from GWAS1, GWAS2, and GWAS3 is shown across the chromosomes. The dotted
362 line indicates the threshold for genome-wide significance ($P < 5 \times 10^{-8}$).

363

364 **Figure 2** Bioinformatic functional interaction network analysis of proteins encoded by all
365 positional candidate genes at all confirmed and suggestive vitiligo candidate loci. As a first step,
366 unsupervised functional interaction network analysis was carried out using STRING v10.0¹¹,
367 considering each protein as a node and permitting ≤ 5 second-order interactions to maximize
368 connectivity. Nodes that shared no edges with other nodes were then excluded from the
369 network. Edge colors are per STRING: teal, interactions from curated databases; purple,
370 experimentally determined interactions; green, gene neighborhood; blue, databases; red, gene
371 fusions; dark blue, gene co-occurrence; pale green, text-mining; black, co-expression; lavender,
372 protein homology. Note that SMEK2 is an alternative name for PPP4R3B.

373

374 **Figure 3** Concordant associations for vitiligo and other autoimmune and inflammatory diseases.
375 We searched the NHGRI-EBI GWAS Catalog and PubMed for associations of the 48 genome-
376 wide significant and 7 suggestive vitiligo susceptibility loci with other autoimmune, inflammatory,
377 and immune-related disorders, and for association with normal human pigmentation variation.
378 Only reported associations that achieved genome-wide significance ($P < 5 \times 10^{-8}$) are included.
379 RA, rheumatoid arthritis; T1D, type 1 diabetes mellitus; AITD, autoimmune thyroid disease;
380 SLE, systemic lupus erythematosus; IBD, inflammatory bowel disease; MS, multiple sclerosis;
381 MG, myasthenia gravis; AI hepatitis, autoimmune hepatitis.

382

383 **Figure 4** Enrichment estimates for functional annotations. The combined CMH GWAS123
384 summary statistics were analyzed using the stratified LD score regression method utilizing the
385 full baseline model⁵¹. Regulatory, yellow; protein coding, blue; intron, green. Bar height
386 represents enrichment which is defined to be the proportion of SNP heritability in the category
387 divided by the proportion of SNPs in that category. Error bars represent jackknife standard error
388 around the enrichment. For each category, percentage of the total markers in the category is in
389 parentheses. Dashed line represents a ratio of 1 (no enrichment). Asterisks indicate enrichment
390 significant at $P < 0.05$ after Bonferroni correction for the 20 categories tested (the categories
391 conserved, repressed, transcribed, and promoter flanking were removed and considered
392 insufficiently specific). CTCF, CCCTC-binding factor; DGF, digital genomic footprint; DHS,
393 DNase hypersensitivity site; TFBS, transcription factor binding site; TSS, transcriptional start
394 site; 5' and 3' UTR, 5' and 3' untranslated regions. H3K4me1, H3K4me3, H3K9ac, and
395 H3K27ac are regulatory chromatin marks^{56,57}.

396

397

Table 1 Allelic associations at vitiligo susceptibility loci following GWAS meta-analysis and replication study

Chr.	Variant	Position (Build 37)	Locus	EA/OA	GWAS123 meta-analysis		GWAS3 replication study		GWAS123 & GWAS3 replication study meta-analysis		Heritability explained* (%)
					<i>P</i> value	Odds ratio	<i>P</i> value	Odds ratio	<i>P</i> value	Odds ratio (95% CI)	
1	rs301807	8484823	<i>RERE</i>	A/G	1.84 x 10 ⁻¹²	1.22	4.09 x 10 ⁻⁰⁴	1.17	4.14 x 10 ⁻¹⁵	1.21 (1.15-1.27)	0.003
1	rs2476601	114377568	<i>PTPN22</i>	A/G	2.21 x 10 ⁻¹⁴	1.39	1.08 x 10 ⁻⁰⁵	1.36	1.21 x 10 ⁻¹⁸	1.38 (1.29-1.49)	0.003
1	rs78037977	172715702	<i>FASLG</i>	G/A	1.39 x 10⁻¹³	1.33	8.95 x 10⁻⁰⁵	1.29	6.74 x 10⁻¹⁷	1.32 (1.24-1.41)	0.003
1	rs16843742	198672299	<i>PTPRC</i>	C/T	8.84 x 10⁻⁰⁹	0.82	1.87 x 10⁻⁰²	0.88	1.02 x 10⁻⁰⁹	0.83 (0.79-0.88)	0.002
2	rs10200159	55845109	<i>PPP4R3B</i>	C/T	3.35 x 10⁻¹³	1.48	3.70 x 10⁻⁰⁷	1.55	3.73 x 10⁻¹⁹	1.51 (1.38-1.66)	0.003
2	rs4308124	112010486	<i>BCL2L11-MIR4435-2HG</i>	C/T	4.99 x 10⁻⁰⁸	1.17	1.67 x 10⁻⁰²	1.12	3.96 x 10⁻⁰⁹	1.15 (1.10-1.21)	0.002
2	rs2111485	163110536	<i>IFIH1</i>	A/G	2.69 x 10 ⁻²²	0.75	8.58 x 10 ⁻⁰⁵	0.83	6.40 x 10 ⁻²⁵	0.77 (0.73-0.81)	0.008
2	rs231725	204740675	<i>CTLA4</i>	A/G	2.25 x 10⁻⁰⁸	1.18	1.57 x 10⁻⁰³	1.16	1.49 x 10⁻¹⁰	1.18 (1.12-1.24)	0.002
2	rs41342147	242407588	<i>FARP2-STK25</i>	A/G	8.03 x 10⁻⁰⁷	0.80	1.25 x 10⁻⁰³	0.80	3.70 x 10⁻⁰⁹	0.80 (0.74-0.86)	0.003
3	rs35161626	23512312	<i>UBE2E2</i>	I/D	7.34 x 10⁻⁰⁷	0.87	1.09 x 10⁻⁰²	0.89	3.13 x 10⁻⁰⁸	0.87 (0.83-0.92)	0.001
3	rs34346645	71557945	<i>FOXP1</i>	A/C	6.11 x 10 ⁻¹⁴	0.80	4.23 x 10 ⁻⁰⁶	0.81	7.99 x 10 ⁻¹⁹	0.80 (0.76-0.84)	0.004
3	rs148136154	119283468	<i>CD80-ADPRH</i>	C/T	5.02 x 10 ⁻¹⁵	1.37	1.74 x 10 ⁻⁰²	1.17	4.58 x 10 ⁻¹⁵	1.31 (1.22-1.40)	0.003
3	rs13076312	188089254	<i>LPP</i>	T/C	3.58 x 10 ⁻²²	1.32	3.48 x 10 ⁻¹⁰	1.33	1.61 x 10 ⁻³⁰	1.32 (1.26-1.38)	0.009
3	rs6583331	196347253	<i>FBXO45-NRROS</i>	A/T	1.39 x 10⁻⁰⁷	0.86	3.62 x 10⁻⁰²	0.91	2.53 x 10⁻⁰⁸	0.87 (0.83-0.92)	0.002
4	rs1031034	102223386	<i>PPP3CA</i>	A/C	4.78 x 10⁻⁰⁶	0.86	2.14 x 10⁻⁰³	0.86	3.43 x 10⁻⁰⁸	0.86 (0.81-0.91)	0.001
6	rs12203592	396321	<i>IRF4</i>	T/C	1.03 x 10⁻⁰⁹	0.77	3.17 x 10⁻⁰⁸	0.68	8.86 x 10⁻¹⁶	0.75 (0.70-0.80)	0.001
6	rs78521699	2908591	<i>SERPINB9</i>	G/A	3.33 x 10⁻⁰⁶	0.79	2.27 x 10⁻⁰³	0.80	2.54 x 10⁻⁰⁸	0.79 (0.73-0.86)	0.001
6	rs60131261	29937335	<i>HLA-A</i>	D/I	2.63 x 10 ⁻⁴⁸	1.53	8.01 x 10 ⁻²⁰	1.54	1.56 x 10 ⁻⁶⁶	1.54 (1.46-1.61)	0.016
6	rs9271597	32591291	<i>HLA-DRB1/DQA1</i>	A/T	3.15 x 10 ⁻⁸⁹	1.77	nd	nd	nd	nd	0.042
6	rs72928038	90976768	<i>BACH2</i>	A/G	1.12 x 10 ⁻¹¹	1.28	2.04 x 10 ⁻⁰⁴	1.25	1.00 x 10 ⁻¹⁴	1.27 (1.19-1.35)	0.003
6	rs2247314	167370230	<i>RNASET2-FGFR1OP- CCR6</i>	C/T	1.97 x 10 ⁻¹³	0.79	1.56 x 10 ⁻⁰⁶	0.79	1.72 x 10 ⁻¹⁸	0.79 (0.75-0.84)	0.003
7	rs117744081	29132279	<i>CPVL</i>	G/A	3.74 x 10⁻²²	1.95	1.88 x 10⁻⁰⁶	1.66	8.72 x 10⁻²⁶	1.84 (1.64-2.06)	0.004
8	rs2687812	133931055	<i>TG-SLA-WISP1</i>	A/T	1.98 x 10 ⁻¹¹	1.21	1.69 x 10 ⁻⁰³	1.15	2.19 x 10 ⁻¹³	1.19 (1.14-1.25)	0.007
9	rs10986311	127071493	<i>NEK6</i>	C/T	5.45 x 10⁻⁰⁷	1.16	5.10 x 10⁻⁰³	1.14	1.01 x 10⁻⁰⁸	1.15 (1.10-1.21)	0.001
10	rs706779	6098824	<i>IL2RA</i>	C/T	1.30 x 10 ⁻²⁴	0.74	9.25 x 10 ⁻⁰⁵	0.84	7.20 x 10 ⁻²⁷	0.77 (0.73-0.81)	0.012
10	rs71508903	63779871	<i>ARID5B</i>	T/C	1.09 x 10⁻⁰⁶	1.18	1.52 x 10⁻⁰³	1.19	6.93 x 10⁻⁰⁹	1.18 (1.12-1.25)	0.001
10	rs12771452	115488331	<i>CASP7</i>	A/G	9.16 x 10 ⁻⁰⁸	0.83	8.42 x 10 ⁻⁰⁶	0.79	4.43 x 10 ⁻¹²	0.82 (0.78-0.87)	0.002
11	rs1043101	35274829	<i>CD44-SLC1A2</i>	G/A	2.08 x 10 ⁻¹³	1.24	4.20 x 10 ⁻⁰⁶	1.24	5.26 x 10 ⁻¹⁸	1.23 (1.18-1.29)	0.003
11	rs12421615	64021605	<i>PPP1R14B-PLCB3-BAD-</i>	A/G	3.38 x 10⁻⁰⁶	1.8 0.87	3.78 x 10⁻⁰³	0.87	4.81 x 10⁻⁰⁸	0.87 (0.83-0.91)	0.001

**GPR137-KCNK4-TEX40-
ESRRA-TRMT112-
PRDX5**

11	rs1126809	89017961	TYR	A/G	7.13 x 10 ⁻³²	0.67	2.54 x 10 ⁻¹³	0.68	1.16 x 10 ⁻⁴³	0.67 (0.63-0.71)	0.012
11	rs11021232	95320808	Gene desert	C/T	1.01 x 10 ⁻²¹	1.38	3.81 x 10 ⁻⁰⁴	1.22	2.10 x 10 ⁻²³	1.34 (1.26-1.41)	0.005
12	rs2017445	56407072	IKZF4	A/G	3.81 x 10 ⁻²⁰	1.31	1.22 x 10 ⁻¹²	1.40	6.62 x 10 ⁻³¹	1.33 (1.27-1.40)	0.005
12	rs10774624	111833788	SH2B3-ATXN2	A/G	1.88 x 10 ⁻¹⁴	0.80	1.52 x 10 ⁻¹⁰	0.75	6.22 x 10 ⁻²³	0.79 (0.75-0.83)	0.004
13	rs35860234	43070206	TNFSF11	G/T	2.82 x 10⁻⁰⁶	1.16	3.45 x 10⁻⁰⁴	1.20	4.76 x 10⁻⁰⁹	1.17 (1.11-1.23)	0.001
14	rs8192917	25102160	GZMB	C/T	1.37 x 10 ⁻¹⁰	1.23	1.23 x 10 ⁻⁰⁶	1.29	8.91 x 10 ⁻¹⁶	1.25 (1.18-1.32)	0.002
15	rs1635168	28535266	OCA2-HERC2	A/C	6.97 x 10 ⁻¹³	1.43	7.45 x 10 ⁻⁰³	1.25	8.78 x 10 ⁻¹⁴	1.37 (1.26-1.49)	0.003
16	rs4268748	90026512	MC1R?	C/T	1.63 x 10 ⁻²⁰	0.73	8.23 x 10 ⁻¹⁵	0.66	2.88 x 10 ⁻³³	0.71 (0.67-0.75)	0.013
17	rs11079035	40289012	KAT2A-HSPB9-RAB5C	A/G	3.20 x 10⁻⁰⁶	1.18	3.19 x 10⁻⁰⁵	1.28	6.77 x 10⁻¹⁰	1.21 (1.14-1.29)	0.001
18	rs8083511	60028655	TNFRSF11A	C/A	9.42 x 10⁻¹⁰	1.24	3.23 x 10⁻⁰²	1.13	2.81 x 10⁻¹⁰	1.21 (1.14-1.28)	0.002
19	rs4807000	4831878	TICAM1	A/G	1.58 x 10⁻⁰⁹	1.19	2.11 x 10⁻⁰⁶	1.24	1.94 x 10⁻¹⁴	1.21 (1.15-1.26)	0.002
19	rs2304206	50168871	SCAF1-IRF3-BCL2L12	A/G	6.45 x 10⁻⁰⁹	0.82	4.52 x 10⁻⁰²	0.90	2.36 x 10⁻⁰⁹	0.84 (0.80-0.89)	0.002
20	rs6059655	32665748	RALY-EIF252-ASIP- AHCY-ITCH	A/G	3.58 x 10⁻¹³	0.63	3.08 x 10⁻⁰⁸	0.57	1.04 x 10⁻¹⁹	0.61 (0.55-0.68)	0.004
20	rs6012953	49123043	PTPN1	G/A	1.18 x 10⁻⁰⁷	1.16	1.74 x 10⁻⁰²	1.11	9.47 x 10⁻⁰⁹	1.15 (1.10-1.20)	0.002
21	rs12482904	43851828	UBASH3A	A/T	5.74 x 10 ⁻²⁹	1.43	1.16 x 10 ⁻⁰³	1.18	5.84 x 10 ⁻²⁹	1.35 (1.28-1.43)	0.010
22	rs229527	37581485	C1QTNF6	A/C	1.40 x 10 ⁻²⁴	1.34	1.15 x 10 ⁻⁰⁷	1.27	1.14 x 10 ⁻³⁰	1.32 (1.26-1.38)	0.006
22	rs9611565	41767486	ZC3H7B-TEF	C/T	1.99 x 10 ⁻¹²	0.78	3.34 x 10 ⁻⁰⁴	0.82	3.13 x 10 ⁻¹⁵	0.79 (0.75-0.84)	0.003
x	rs73456411	29737404	IL1RAPL1	T/G	1.57 x 10⁻⁰⁷	1.72	5.90 x 10⁻⁰³	1.62	7.34 x 10⁻¹⁰	1.77 (1.47-2.13)	0.001
x	rs5952553	49392721	CCDC22-FOXP3-GAGE	C/T	1.81 x 10 ⁻⁰⁸	0.85	3.48 x 10 ⁻⁰²	0.92	1.05 x 10 ⁻⁰⁹	0.86 (0.82-0.90)	0.001

*Heritability explained by all independent signals of the locus. Chr., chromosome; CI, confidence interval; nd, not determined; EA, effect allele; OA, other allele. Bold, novel significant vitiligo susceptibility loci. The chromosome 16 association peak spans a large number of genes, including *MC1R*.

398

399

400 **ONLINE METHODS**

401
402
403 **Subjects**

404 The genome-wide portion of this study included unrelated cases from our three generalized
405 vitiligo GWAS: GWAS1⁴ (n = 1514), GWAS2⁶ (n = 450), and the current GWAS3 (n = 1090). All
406 cases were of non-Hispanic-Latino European-derived white ancestry (EUR) from North America
407 and Europe, and met strict clinical criteria for generalized vitiligo⁵⁹. All controls were EUR
408 individuals not specifically known to have any autoimmune disease or malignant melanoma, for
409 whom genome-wide genotypes were obtained from the NCBI database of Genotypes and
410 Phenotypes (dbGaP; phs000092.v1.p1, phs000125.v1.p1, phs000138.v2.p1, phs000142.v1.p1,
411 phs000168.v1.p1, phs000169.v1.p1, phs000206.v3.p2, phs000237.v1.p1, phs000346.v1.p1,
412 and phs000439.v1.p1 for GWAS1; phs000203.v1.p1, and phs000289.v2.p1 for GWAS2;
413 phs000196.v2.p1, phs000303.v1.p1, phs000304.v1.p1, phs000368.v1.p1, phs000381.v1.p1,
414 phs000387.v1.p1, phs000389.v1.p1, phs000395.v1.p1, phs000408.v1.p1, phs000421.v1.p1,
415 phs000494.v1.p1, and phs000524.v1.p1 for GWAS3). Control datasets were matched to each of
416 the three GWAS case datasets based on platforms used for genotyping. The independent
417 replication study included 1827 unrelated EUR vitiligo cases and 2181 unrelated EUR controls
418 not included in any of the GWAS. All subjects provided written informed consent. This study was
419 carried out under the jurisdiction of each local IRB with overall oversight of the Colorado Multiple
420 Institutional Review Board (COMIRB).

421

422 **Genome-wide genotyping**

423 Saliva specimens were obtained using a DNA self-collection kit (Oragene, DNA Genotek), and
424 DNA was prepared using either the Maxwell apparatus/16 LEV Blood DNA kit (Promega) or
425 the DNA Genotek Oragene Purifier protocol. DNA concentrations were measured using either
426 the Qubit dsDNA BR Assay kit and Qubit 2.0 Fluorometer (Invitrogen) or the Promega

427 QuantiFluor ONE dsDNA kit and GloMax®-Multi+ Detection System (Promega).

428 Genome-wide genotyping for the GWAS3 cases was performed for 716,503 variants
429 using Illumina Human OmniExpress BeadChips by the Center for Inherited Disease Research
430 (CIDR). Genotype data for GWAS3 were deposited in dbGaP (phs000224.v3.p1). GWAS1⁴
431 and GWAS2⁶ have been described previously.

432

433 **Genome-wide quality control procedures**

434 Quality control filtering of genome-wide genotype data was carried out using PLINK⁶⁰, version
435 1.9. For each case/control dataset, DNA strand calls were reversed as needed. Cases were
436 excluded on the basis of SNP call rates <98.5%, discordance between reported and observed
437 sex, or inadvertent subject duplication, and controls were excluded on the basis of SNP call
438 rates < 98%. SNPs were excluded on the basis of genotype missing rate > 2% for SNPs with
439 observed minor allele frequency (MAF) ≥ 0.01 , and for SNPs with MAF < 0.01 exclusion
440 criteria were genotype missing rate >1% and < 5 minor alleles observed, or significant ($P <$
441 10^{-4}) deviation from Hardy-Weinberg equilibrium. For X chromosome SNPs, Hardy-Weinberg
442 equilibrium tests were performed in females, and SNPs with $P < 10^{-4}$ were excluded from the
443 final analysis. For each GWAS, only SNPs that existed in all case and control datasets were
444 retained for imputation.

445 Within each GWAS, subjects were excluded based on cryptic relatedness identified by
446 pairwise identity-by-descent estimations ($\pi\text{-hat} > 0.0625$), in which case the individual with
447 lower SNP call rate was excluded. For each of the three GWAS, the cleaned case dataset was
448 combined with one cleaned control dataset at a time and the genotype data of 270 subjects of
449 Phase I and II of the International HapMap Project from 4 populations, and principal
450 components analysis (PCA) was performed with EIGENSOFT⁵⁹ based on tag-SNPs (within
451 which no pair were correlated with $r^2 > 0.2$) selected from genotyped SNPs. The first two
452 eigenvectors were used to produce a PCA plot. A PCA plot was first made for cases and

453 HapMap samples, and cases that were clearly separated from the main cluster of cases and
454 HapMap EUR samples were excluded as outliers. A PCA plot of controls and HapMap
455 samples was then made, and the same x and y coordinates that separated the case outliers
456 from the main cluster of cases and HapMap EUR samples were used to identify control
457 outliers.

458 After all QC procedures, the final number of genotyped SNPs remaining in GWAS1,
459 GWAS2, and GWAS3 were 464,902, 494,043, and 483,609, respectively. For autosomal
460 analyses, the final numbers of cases and controls in GWAS1, GWAS2, and GWAS3 were
461 1,381 and 14,518, 413 and 5,209, and 1,059 and 17,678, respectively, whereas for X
462 chromosome analyses, the final numbers of cases and controls in GWAS1, GWAS2, and
463 GWAS3 were 1,380 and 9,439, 413 and 5,209, and 1,059 and 14,220, respectively. This
464 sample size provided at least 85% power to detect associations with $OR \geq 1.22$ at genome-
465 wide significance ($P = 5 \times 10^{-8}$) for $MAF \geq 0.25$.

466

467 **Genome-wide Genotype Imputation**

468 For each GWAS, we used SHAPEIT version2 to pre-phase genotypes to produce best-guess
469 haplotypes, and then performed imputation with these estimated haplotypes using IMPUTE2
470 and the 1000 Genomes Project phase I integrated variant set version 3 (March, 2012) as the
471 reference panel. All cryptic related individuals and outliers from each GWAS were included in
472 the process to improve imputation accuracy, but were removed for the final analyses. Only
473 genotypes with imputation INFO > 0.5 were retained, which were combined with prior SNP
474 genotype data. Imputed genotypes for variants with $MAF \geq 0.01$ calculated from all 3 GWAS
475 combined and without significant ($P > 10^{-5}$) deviation from Hardy-Weinberg equilibrium were
476 used in the final analysis, which included 8,721,242 autosome variants and 245,169
477 chromosome X variants.

478

479 **Replication study genotyping and quality control procedures**

480 For the replication study, genotyping was attempted for 379 variants using a custom Illumina
481 GoldenGate array by CIDR. 71 SNPs were excluded on the basis of genotype missing rate > 2%
482 (which includes apparent technical failures), or significant ($P < 10^{-4}$) deviation from Hardy-
483 Weinberg equilibrium. For X chromosome SNPs, Hardy-Weinberg equilibrium tests were
484 performed in females. Subjects were excluded on the basis of SNP call rates <95%, or
485 discordance between reported and observed sex. Unintended duplicate samples were identified
486 by pairwise identity-by-descent estimations ($\pi\text{-hat} > 0.99$), in which case the individual with
487 lower SNP call rate was excluded. The final numbers of remaining cases and controls were
488 1,827 and 2,181, respectively, providing at least 80% power to replicate associations at $P = 0.05$
489 with Bonferroni correction for up to 48 independent tests for $OR \geq 1.23$ for $MAF \geq 0.25$.

490

491 **Statistical analyses**

492 To control for the effects of population stratification, we assigned cases and controls of each
493 GWAS to homogenous clusters using GemTools⁶⁰, and performed Cochran-Mantel- Haenszel
494 (CMH) analysis to test for association for each GWAS and the combined GWAS data, with the
495 cluster variable defined by the case-control clusters from each GWAS. After removing variants
496 within the extended MHC, the genomic inflation factor for GWAS1, GWAS2, and GWAS3 was
497 1.068, 1.059, and 1.013, respectively. For the combined GWAS1-GWAS2-GWAS3 genotype
498 data for shared SNPs, the genomic inflation factor was 1.019.

499 For the replication study, after quality control procedures we compared allele
500 frequencies for the remaining 308 SNPs in the remaining 1,827 cases and 2,181 controls using
501 the Cochran-Armitage trend test. ORs and 95% confidence limits were calculated by logistic
502 regression analysis. We used CMH analysis to obtain ORs and P values for the combined
503 GWAS plus the replication study data, with the cluster variable defined by the case-control
504 clusters from each GWAS and the replication study data as one cluster. To analyze X

505 chromosome SNPs, we assumed complete X-inactivation and similar effect size between
506 males and females, with the effect of having an A allele in a male equal to the effect of having
507 two A alleles in a female⁶³. We thus coded males as homozygous for the allele carried for each
508 variant and tested for association by CMH analysis to obtain ORs and P values for each
509 GWAS, the combined GWAS, and the combined GWAS plus the replication study data, and by
510 the Cochran- Armitage trend test for the replication study data.

511 To test heterogeneity of associations across the three GWAS and the replication study
512 data, we performed the Cochran Q test. The analysis was done with PLINK, version 1.07,
513 using the ORs and standard errors estimated from the CMH analysis of each GWAS, and from
514 logistic regression analysis of the replication study data. The I^2 statistic from the Q test
515 quantifies heterogeneity and ranges from 0% to 100%⁶⁴, with a value of 75% or greater
516 typically taken to indicate a high degree of heterogeneity⁶⁵.

517 To test for multiple independent signals at each locus, we performed logistic regression
518 analysis of each locus conditional on the most significantly associated variant, including as
519 covariates in the model the significant principal components for each GWAS derived from
520 GemTools⁶² to control for population stratification, and used a stepwise procedure to select
521 additional variants, one by one, until no additional variants showed conditional P values $\leq 1.0 \times$
522 10^{-5} . If a tested variant and the conditional variant could not improve each other significantly (P
523 ≥ 0.05 when comparing the two SNP model to a single SNP model), then both variants were
524 considered to represent the same signal. We calculated the variance explained by a specific
525 variant or a set of variants from the combined GWAS as the Pseudo R^2 of a logistic regression
526 model which included the specific variants tested.

527

528 **Bioinformatic pathway and functional enrichment analyses**

529 To screen for functional relationships among the vitiligo candidate genes, we carried out
530 pathway analysis of the protein products of all positional candidate genes at all 48 confirmed

531 loci and the seven suggestive loci using g:PROFILER¹⁰, PANTHER¹¹, and STRING¹². To
532 assess enrichment of association signals in different functional genomic categories contributing
533 to vitiligo heritability, we applied stratified LD score regression⁵¹ to the combined CMH
534 GWAS123 summary statistics. The regression model contained 24 overlapping functional
535 categories, including coding, UTR, promoter and intronic regions, annotations for different
536 histone marks, DNase I hypersensitivity site (DHS) regions, combined ChromHMM and Segway
537 predictions, conserved regions in mammals, super-enhancers and FANTOM5 enhancers. For
538 each of the 24 categories, a 500-bp window was used. Linkage disequilibrium data were
539 provided by the LD score software, estimated from the EUR samples in the 1000 Genomes
540 Project Phase 1. Enrichment per category was calculated by the ratio of the estimated
541 proportion of heritability explained by the category over the proportion of the markers in the
542 category.

543

544 **PrediXcan and Monocyte eQTL Co-Localization analyses**

545 We carried out a gene-based test of association of vitiligo with “imputed” expression profiles for
546 11,553 autosomal genes in whole blood using PrediXcan⁵⁸. The analysis included 2,853 cases
547 and 37,412 controls from the combined GWAS. Association testing between expression
548 estimates for each gene and affection status for vitiligo was performed by generalized logistic
549 regression. *P* values were adjusted for the number of genes tested ($n = 11,553$). *NRROS*,
550 *ZC3H7B*, *TNFRSF11A*, *BCL2L12*, *RALY*, *ASIP*, *OCA2*, and *TYR* were excluded from the
551 PrediXcan analysis due to poor prediction of gene expression in blood cells.

552 We derived expression quantitative trait loci (eQTLs) in peripheral blood monocytes from
553 414 EUR subjects with paired genotyping and gene expression data⁶⁶. SHAPEIT version2 was
554 used to pre-phase genotypes to produce best-guess haplotypes with imputation performed
555 using IMPUTE2 and the 1000 Genomes Project phase I integrated variant set version 3 (March,
556 2012) as reference panel. We tested for co-localization of eQTL and vitiligo GWAS autosomal

557 association patterns as described^{67,68}. Vitiligo susceptibility loci were defined by windows of
558 robust association plus an added 100 kb buffer on both sides. eQTL probes were selected by
559 choosing probes that resided within these windows. Probe quality annotation was performed
560 using ReMOAT⁶⁹ and all probes with an annotation of “bad” were removed. After removing non-
561 autosomal loci and duplicate probe IDs, a total of 904 probes remained. All vitiligo susceptibility
562 loci contained at least one probe with the exception of the gene desert 3’ of *TYR*, for which the
563 only probe that intersected the locus was excluded due to ReMOAT annotation of “bad”. Within
564 each locus window, all SNPs were tested for association with all probes using linear regression.
565 P values, MAF for each SNP and respective sample sizes were used as input to test for co-
566 localization, simultaneously testing five mutually exclusive hypotheses by generating 5
567 corresponding posterior probabilities (PP):

- 568 • H0 (PP0): There is no association with either the GWAS or the eQTL.
- 569 • H1 (PP1): There is association for the GWAS only.
- 570 • H2 (PP2): There is association for the eQTL only.
- 571 • H3 (PP3): There is association for both the GWAS and the eQTL, but the associated
572 variants are different for the GWAS and the eQTL.
- 573 • H4 (PP4): The associated variants are the same for both the GWAS and the eQTL (co-
574 localization).

575 Posterior probabilities were calculated using the R package “coloc” using default settings for
576 prior probabilities of association. Co-localization was assessed as per Guo *et al.*⁶⁸; significant
577 co-localization was $PP_3+PP_4 > 0.99$ and $PP_4:PP_3 > 5$, and suggestive co-localization was
578 $PP_3+PP_4 > 0.95$ and $PP_4:PP_3 > 3$.

579

580 **URLs.** 1000 Genomes Project, <http://www.1000genomes.org/>; coloc, [https://cran.r-](https://cran.r-project.org/web/packages/coloc/index.html)
581 [project.org/web/packages/coloc/index.html](https://cran.r-project.org/web/packages/coloc/index.html); GemTools,
582 <http://wpicr.wpic.pitt.edu/WPICCompGen/GemTools/GemTools.htm>; IMPUTE2,

583 https://mathgen.stats.ox.ac.uk/impute/impute_v2.html; International HapMap Project,
584 <http://hapmap.ncbi.nlm.nih.gov/>; PrediXcan, <https://github.com/hriordan/PrediXcan>; SHAPEIT,
585 <http://www.shapeit.fr/>; REMOAT, <http://remoat.sysbiol.cam.ac.uk/transcript.php>.

586

587 **Methods-only References**

588 59. Taïeb, A. & Picardo, M. The definition and assessment of vitiligo: a consensus report of the
589 VitiligoEuropean Task Force. *Pigment Cell Res.* **20**, 27-35 (2007).

590 60. Purcell, S. *et al.* PLINK: a toolset for whole-genome association and population-based
591 linkage analysis. *Am. J. Hum. Genet.* **81**, 559–575 (2007).

592 61. Price, A.L. *et al.* Principal components analysis corrects for stratification in
593 genome-wide association studies. *Nat. Genet.* **38**, 904–909 (2006).

594 62. Lee, A.B., Luca, D., Klei, L., Devlin, B. & Roeder, K. Discovering genetic ancestry using
595 spectral graph theory. *Genet. Epidemiol.* **34**, 51–59 (2010).

596 63. Chang, D. *et al.* Accounting for eXentricities: analysis of the X chromosome in GWAS
597 reveals X- linked genes implicated in autoimmune diseases. *PLoS One* **9**, e113684
598 (2014).

599 64. Higgins, J.P. & Thompson, S.P. Quantifying heterogeneity in a meta-analysis. *Stat. Med.* **21**,
600 1539–1558 (2002).

601 65. Higgins, J.P. *et al.* Measuring inconsistency in meta-analyses. *Br. Med. J.* **327**, 557–560
602 (2003).

603 66. Fairfax, B.P. *et al.* Innate immune activity conditions the effect of regulatory variants upon
604 monocyte gene expression. *Science* **343**, 1246949 (2014).

605 67. Giambartolomei, C. *et al.* Bayesian test for colocalisation between pairs of genetic
606 association studies using summary statistics. *PLoS Genet.* **10**, e1004383 (2014).

607 68. Guo, H. *et al.* Integration of disease association and eQTL data using a Bayesian
608 colocalisation approach highlights six candidate causal genes in immune-mediated

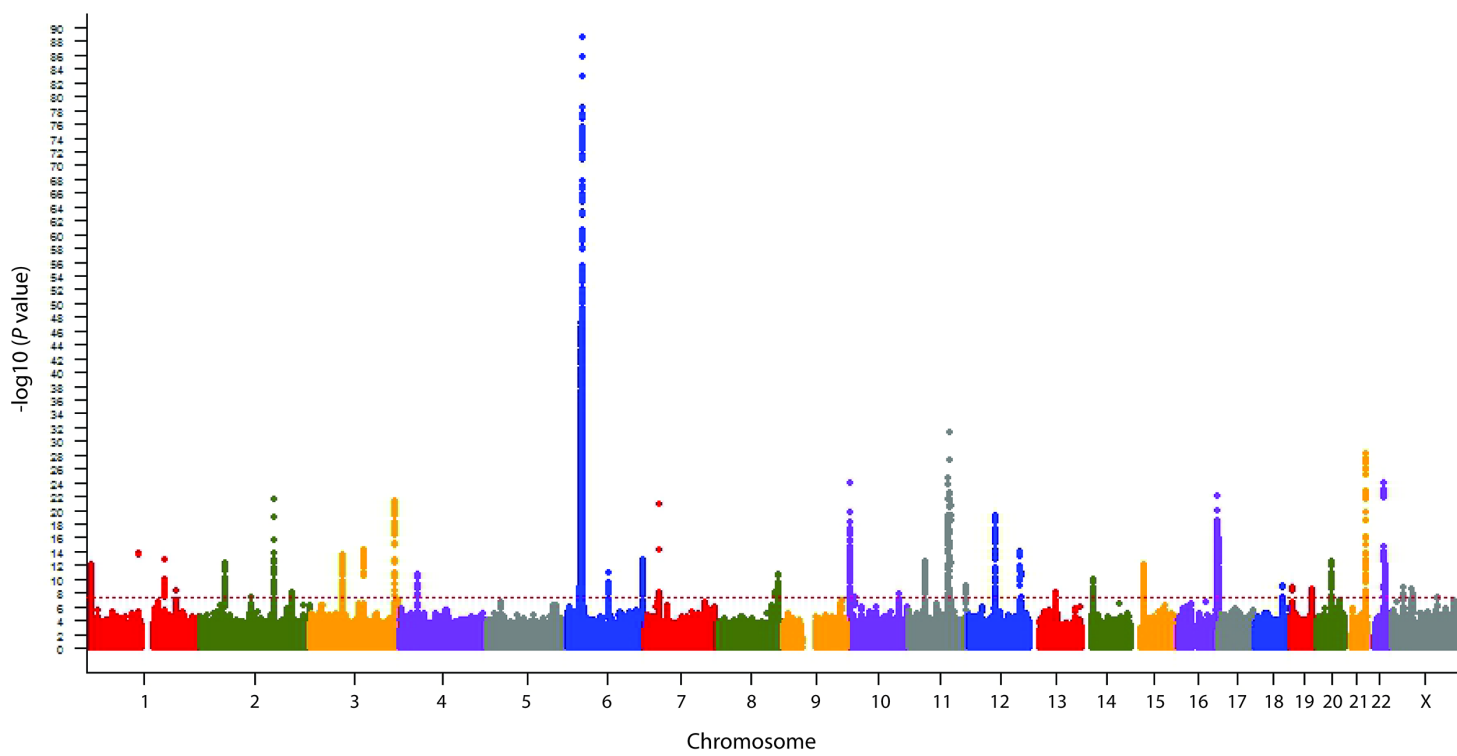
- 609 diseases. *Hum. Mol. Genet.* **24**, 3305-3313 (2015).
- 610 69. Arloth, J., Bader, D.M., Röh, S. & Altmann, A. Re-Annotator: Annotation pipeline for
- 611 microarray probe sequences. *PLoS One.* **10**, 1–13 (2015).
- 612

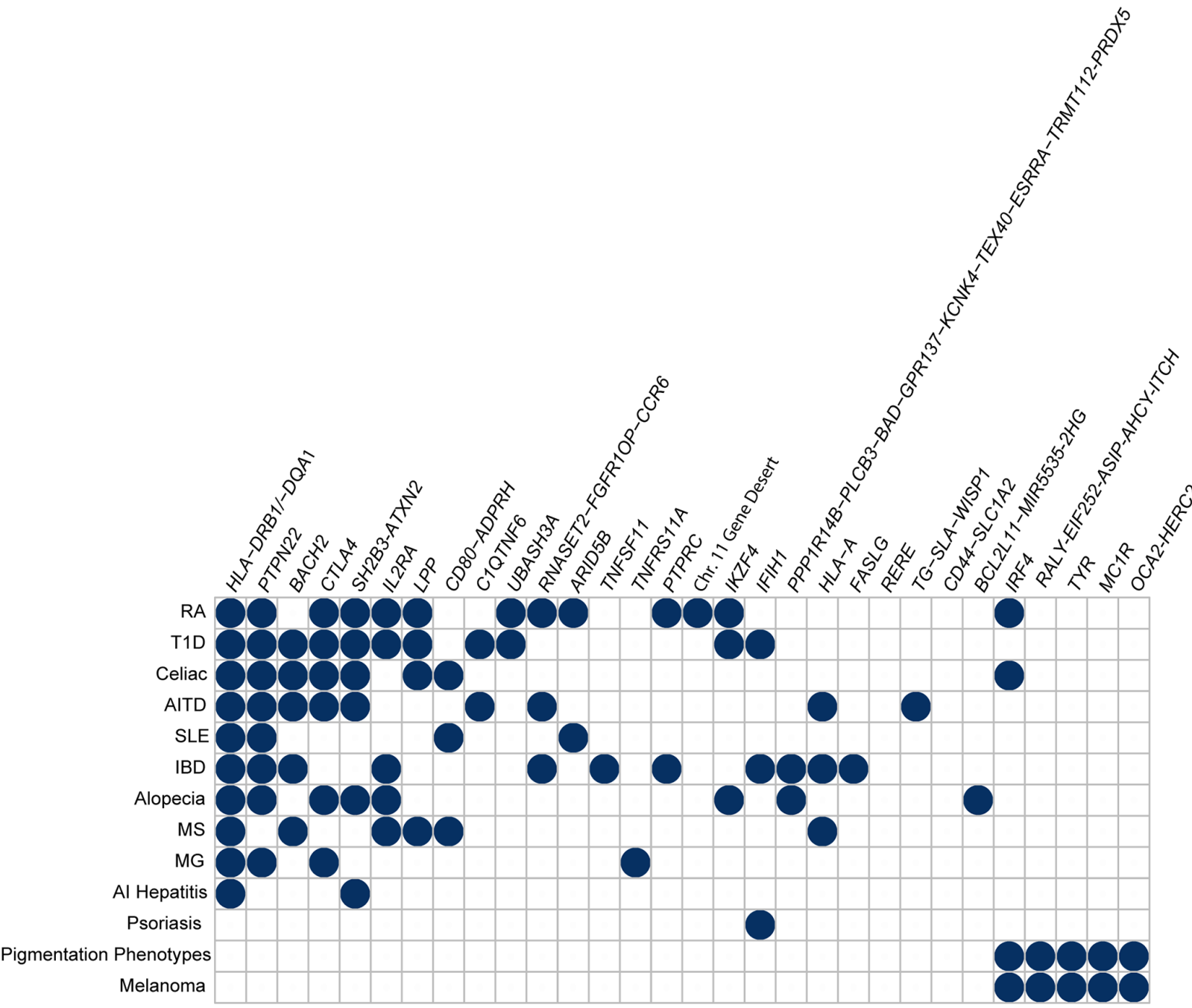
613 **Competing Financial Interests**

614 The authors declare no competing financial interests.

615

616





Enrichment=(prop. heritability)/(prop. markers)

